Published in final edited form as:
Aging Cell. 2010 December ; 9(6): 1047–1056. doi:10.1111/j.1474-9726.2010.00631.x.

The telomeric protein SNM1B/Apollo is required for normal cell proliferation and embryonic development

Shamima Akhter[1], **Yung C. Lam**[1], **Sandy Chang**[1,2,*], and **Randy J. Legerski**[1]

[1]Department of Genetics, The U.T. M.D. Anderson Cancer Center, 1515 Holcombe Blvd, Houston, TX 77030, USA

[2]Department of Hematopathology, The U.T. M.D. Anderson Cancer Center, 1515 Holcombe Blvd, Houston, TX 77030, USA

Summary

Conserved metallo β-Lactamase and β-CASP (CPSF-Artemis-Snm1-Pso2) domain nuclease family member SNM1B/Apollo is a shelterin-associated protein that localizes to telomeres through its interaction with TRF2. To study its *in vivo* role, we generated a knockout of *SNM1B/Apollo* in a mouse model. *Snm1B/Apollo* homozygous null mice die at birth with developmental delay and defects in multiple organ systems. Cell proliferation defects were observed in *Snm1B/Apollo* mutant mouse embryonic fibroblasts (MEFs) owing to high levels of telomeric end-to-end fusions. Deficiency of the nonhomologous end-joining (NHEJ) factor *Ku70*, but not *p53*, rescued the developmental defects and lethality observed in *Snm1B/Apollo* mutant mice as well as the impaired proliferation of *Snm1B/Apollo*-deficient MEFs. These findings demonstrate that *SNM1B/Apollo* is required to protect telomeres against NHEJ-mediated repair, which results in genomic instability and the consequent multi-organ developmental failure. Although *Snm1B/Apollo*-deficient MEFs exhibited high levels of apoptosis, abrogation of p53-dependent programmed cell death did not rescue the multi-organ developmental failure in the mice.

Keywords

chromosome instability; Ku; mouse model; nonhomologous end-joining; SNM1B/Apollo; telomeres

Correspondence: Randy J. Legerski, Department of Genetics, The U.T. M.D. Anderson Cancer Center, 1515 Holcombe Blvd, Houston, TX 77030, USA. Tel.: +1 713 834 6363; fax: +1 713 792 1474; rlegersk@mdanderson.org.
*Present address: Department of Laboratory Medicine, Yale University School of Medicine, 330 Cedar St., New Haven, CT 06511, USA.

Author contributions

Conceived and designed the experiments: SA, YCL, SC, RJL. Performed the experiments: SA, YCL. Analyzed the data: SA, YCL, SC, RJL. Wrote the article: SA, SC, RJL.

Supporting Information

Additional supporting information may be found in the online version of this article:
Fig. S1 Effect of *Trp53*-deficiency on *Snm1B/Apollo*$^{-/-}$ embryo development.
As a service to our authors and readers, this journal provides supporting information supplied by the authors. Such materials are peer-reviewed and may be re-organized for online delivery, but are not copy-edited or typeset. Technical support issues arising from supporting information (other than missing files) should be addressed to the authors.

Introduction

SNM1/Apollo is a member of the *SNM1* (Sensitivity to Nitrogen Mustard) or *PSO2* (sensitivity to *PSO*ralen) gene family that encodes proteins involved in RNA processing, DNA metabolism, and cell cycle regulation (Cattell *et al.*, 2010; Yan *et al.*, 2010). The common features of this family are a metallo-β-lactamase (MBL) fold and an appended β-CASP (CPSF-Artemis-Snm1-Pso2) domain (Moshous *et al.*, 2001; Callebaut *et al.*, 2002), which together have been shown to constitute a nuclease activity in the SNM1 proteins (Ma *et al.*, 2002; Pannicke *et al.*, 2004; Li *et al.*, 2005; Lenain *et al.*, 2006; Hejna *et al.*, 2007; Povirk *et al.*, 2007; Hazrati *et al.*, 2008; Yannone *et al.*, 2008; Weterings *et al.*, 2009). The founding member of the family, SNM1, was discovered in budding yeast (Henriques & Moustacchi, 1980; Ruhland *et al.*, 1981) and has a singular role in the repair processing of DNA interstrand cross-links (ICLs), but not in the repair of double-strand breaks (DSBs) or monoadducts (Magana-Schwencke *et al.*, 1982; Wilborn & Brendel, 1989; Li & Moses, 2003; Barber *et al.*, 2005). The mammalian ortholog Artemis has been shown to have roles in V(D)J recombination, repair of DSBs by both nonhomologous end joining (NHEJ) and homologous recombination, and in cell cycle regulation in response to DNA damage (Moshous *et al.*, 2001; Ma *et al.*, 2002; Riballo *et al.*, 2004; Zhang *et al.*, 2004; Geng *et al.*, 2007; Beucher *et al.*, 2009). A second mammalian ortholog SNM1A has roles in mediating resistance to some cross-linking drugs and in regulating cell cycle checkpoints in response to DNA damage and spindle poisons (Dronkert *et al.*, 2000; Akhter *et al.*, 2004; Ahkter *et al.*, 2005; Akhter & Legerski, 2008). SNM1B/Apollo has been shown to have a variety of roles in cellular metabolism including the repair of ICLs and in mediating a mitotic checkpoint in response to spindle poisons (Demuth *et al.*, 2004; Bae *et al.*, 2008; Liu *et al.*, 2009). In addition, a number of laboratories have reported that SNM1B/Apollo interacts with the telomere-binding protein TRF2 and has a role in telomere maintenance (Freibaum & Counter, 2006; Lenain *et al.*, 2006; van Overbeek & de Lange, 2006; Chen *et al.*, 2008; Demuth *et al.*, 2008). TRF2 is a member of the shelterin complex (de Lange, 2005), which protects telomeres from the activation of the DNA damage response (DDR) and the resulting end-to-end joining of chromosomes (Denchi & de Lange, 2007). Likewise, depletion of SNM1B/Apollo by siRNA was also shown to lead to the activation of a DDR at telomeres and increased levels of chromosomal end-to-end fusions when TRF2 was also removed (Lenain *et al.*, 2006). Toward the goal of elucidating a fuller understanding of the cellular role of *SNM1B/Apollo*, we used a gene-targeting strategy to knockout its function in a mouse model. In work to be reported elsewhere (Lam *et al.*, 2010), we have made a thorough analysis of the defect in telomere maintenance in *Snm1B/Apollo* null cells. These studies confirm that in the absence of SNM1B/Apollo, telomeric end-to-end fusions are greatly elevated because of the activation of the DDR. Furthermore, this phenotype is a result of a requirement for the nuclease function of *SNM1B/Apollo* to resect leading strand telomeres to create 3′ overhangs necessary for telomere protection. Here, we report on the consequences of the knockout of *Snm1B/Apollo* to the developing embryo and the effects on cellular proliferation.

Results

Snm1B/Apollo-deficient mice, a perinatal lethality

To examine the function of *SNM1B/Apollo* in an animal model, we generated *Snm1B/Apollo* knockout mice. The design of the targeting construct by which exon 4 was deleted from *Snm1B/Apollo* and replaced by the pGK-neo cassette to generate a disruption of the gene in mouse ES cells has been previously reported (Lam *et al.*, 2010). Deletion of exon 4 eliminated over 66% of the *Snm1B/Apollo* coding region, which includes the β-CASP domain, the nuclear localization site, and the TRF2 binding site. Here, we describe the phenotypic consequences of the disruption of *SNM1B/Apollo* in this mouse model.

Heterozygous *Snm1B/Apollo* mice exhibited apparent normal development and were viable and fertile. Analysis of crosses between heterozygous mice, on a B6/129 mixed genetic background, showed that 100% of *Snm1B/Apollo* homozygous mutants died immediately around the time of birth indicating a perinatal lethal phenotype (Table 1).

Snm1B/Apollo is essential for normal murine embryogenesis

To investigate the perinatal lethality of *Snm1B/Apollo* embryos, timed heterozygous matings were performed, and females were sacrificed from E11.5 to E19.5. All embryos were alive at the different stages of embryogenesis (Table 2). The *Snm1B/Apollo*$^{-/-}$ embryos displayed no overt gross structural defects; however, they were strikingly smaller than *Snm1B/Apollo*$^{+/+}$ or *Snm1B/Apollo*$^{+/-}$ embryo littermates during all developmental stages examined (Fig. 1A). The average body weight of *Snm1B/Apollo*$^{-/-}$ embryos at E16.5 was 0.222 ± 0.019 g (n = 4), which was ~40% of the body weight of wild-type 0.545 ± 0.012 g (n = 6) or heterozygous 0.539 ± 0.11 g (n = 14) littermates. Histological analyses performed on day E13.5, E16.5, and E18 *Snm1B/Apollo*$^{-/-}$ embryos revealed a global developmental impairment because of hypocellularity in almost all organs (Fig. 1B–E). All *Snm1B/Apollo*$^{-/-}$ embryos died at the postnatal (P0) stage. Analysis of brain and lungs at this stage by H&E staining revealed that the mutant brains were hypocellular, and that the normal laminar arrangement of cells in the cortex was disrupted (Fig. 1C). Histological analysis of the lungs of E16.5 *Snm1B/Apollo*$^{-/-}$ mutant embryos showed enlarged alveolar cells lining the bronchioles of *Snm1B/Apollo*$^{-/-}$ lungs with marked pleomorphism compared to wild-type controls (Fig. 1E). This immature lung phenotype is suggestive of respiratory distress. In addition, we also found that the *Snm1B/Apollo*$^{-/-}$ thymus was markedly hypocellular (Fig. 1D). The endocardial cushions of the heart were prominent and poorly differentiated, consisting of immature-appearing mesenchymal cells. In some areas, gut epithelium (small intestine) was disorganized with piling up and atypia of columnar epithelium in the gut (data not shown). Together, this cellular morphology suggests that there is a delay or arrest in development in *Snm1B/Apollo*$^{-/-}$ embryos that affects multiple organ systems.

Snm1B/Apollo deficiency causes a cell proliferation defect

The common developmental defect observed in *Snm1B/Apollo* homozygous embryos appears to be a generalized reduction in body size and hypocellularity compared with their control littermates that could be because of defect in cell proliferation. Therefore, we established primary mouse embryonic fibroblast (MEF) cultures from wild-type and homozygous mutant mice at E13.5 to investigate their growth potential. Using the 3T3 proliferation protocol (Todaro & Green, 1963), quantitative studies on the growth of MEFs in culture and their development into established lines were conducted. *Snm1B/Apollo*$^{-/-}$ mutant MEFs grew very poorly compared to wild-type MEFs (Fig. 2A), indicating that under tissue culture conditions, *SNM1B/Apollo* has a role in promoting normal cell growth.

To determine the basis of the proliferative defect observed in *Snm1B/Apollo* mutant MEFs, we examined a number of parameters of cell growth. Cell cycle analysis indicated that sub-G1 cells had increased approximately 60-fold in *Snm1B/Apollo*$^{-/-}$ MEFs compared to wild-type cells at passage 3, indicating a high level of apoptosis in the mutant cells (Fig. 2B). The status of replicating (S phase) cells was analyzed by BrdU incorporation at cell passage number three. BrdU staining showed a dramatic reduction in the S-phase population of up to 80–85% in *Snm1B/Apollo*$^{-/-}$ mutant MEFs compared to wild-type cells (Fig. 2C). We also examined two parameters of aberrant cell growth and observed that *Snm1B/Apollo*$^{-/-}$ MEFs had dramatically increased levels of tetraploid (Fig. 2D) and binucleated cells (Fig. 2E) compared to wild-type MEFs. Finally, we also examined cell proliferation in embryos by injecting pregnant females with BrdU. In contrast to the high level of S-phase cells observed

in *Snm1B/Apoll*$^{+/+}$ embryos, a dramatically lower level was observed in *Snm1B/Apollo*$^{-/-}$ embryos (Fig. 3A). The Ki-67 protein (also known as MKI67) is a recognized cellular marker for cellular proliferation (Scholzen & Gerdes, 2000). Examination of this marker in embryonic tissues also revealed a strong proliferation defect in the *Snm1B/Apollo*$^{-/-}$ embryos (Fig. 3B). Taken together, these findings suggest that genomic instability and increased apoptosis account for the proliferation defects observed in *Snm1B/Apollo* null cells.

Snm1B/Apollo$^{-/-}$ MEFs exhibit telomeric fusions

SNM1B/Apollo has been previously implicated in telomere protection during S phase of the cell cycle via an interaction with the shelterin component TRF2 (Freibaum & Counter, 2006; Lenain *et al.*, 2006; van Overbeek & de Lange, 2006; Chen *et al.*, 2008; Demuth *et al.*, 2008). To investigate whether the observed proliferation defects may be the result of telomere end-to-end fusions, we examined metaphase spreads of primary (passage 2) MEFs derived from *Snm1B/Apollo*$^{+/+}$ and *Snm1B/Apollo*$^{-/-}$ embryos. In contrast to *Snm1B/Apollo*$^{+/+}$ and *Snm1B/Apollo*$^{+/-}$ MEFs, approximately 90% of all *Snm1B/Apollo*$^{-/-}$ displayed highly aberrant metaphases (Fig. 4A,B). The mutant cells also exhibited a high level of end-to-end chromosome fusions including p-p, p-q, and q-q arm fusions (Fig. 4C, left panel). Telomere FISH revealed that fusions were accompanied by telomere signals at fusion sites (Fig. 4C, right panel). These results suggest that a high degree of chromosomal instability occurs in the absence of SNM1B/Apollo, and this phenotype likely contributes to the proliferation defects observed in Snm1B/Apollo MEFs.

Ku70, but not p53, deficiency rescues the proliferation defect and lethality of *Snm1B/Apollo*$^{-/-}$ mice

The cell proliferation defects described previously including slow growth, apoptosis, and reduced S-phase population in *Snm1B/Apollo*$^{-/-}$ cells indicate that *SNM1B/Apollo* is essential for normal cellular progression. In many cases, it has been observed that a cross with p53-deficient mice can rescue embryonic lethality associated with extensive apoptosis as a result of excessive DNA damage (Gao *et al.*, 2000). To determine whether p53 deficiency can rescue the observed defects in *Snm1B/Apollo*$^{-/-}$ embryos, we performed a series of crosses with *Trp53*$^{-/-}$ mice and generated *Snm1B/Apollo*$^{+/-}$ *Trp53*$^{-/-}$ and *Snm1B/Apollo*$^{-/-}$ *Trp53*$^{-/-}$ genotypes. We found that *Snm1B/Apollo p53* double-homozygous mutant embryos exhibited a reduced body size and died shortly after birth similar to *Snm1B/Apollo*$^{-/-}$ mice (Fig. S1). We conclude that the developmental defects and perinatal lethality of *Snm1B/Apollo*$^{-/-}$ mice were not rescued by the loss of *p53*.

The telomeric fusions described previously (Fig. 4) and elsewhere (Lam *et al.*, 2010) appear to be mediated by the NHEJ pathway of DSB repair. Ku, which is a core component of the NHEJ pathway, is a heterodimer composed of Ku70 and Ku80. *Ku70* null mice are viable but exhibit a reduced size and shortened lifespan (Guo *et al.*, 2007). To examine the effect of *Ku70* deficiency on the *Snm1/Apollo* phenotype, we performed crosses to generate *Snm1B/Apollo*$^{-/-}$ *Ku70*$^{-/-}$ mice. Interestingly, the loss of *Ku70* resulted in the rescue of the perinatal lethality of the *Snm1B/Apollo*$^{-/-}$ embryos. The *Snm1B/Apollo*$^{-/-}$ *Ku70*$^{-/-}$ mice were viable and exhibited a survival curve highly similar to *Ku70*$^{-/-}$ mice (Fig. 5A). The proliferation defect observed in *Snm1B/Apollo*$^{-/-}$ MEFs was largely rescued in the *Snm1B/Apollo*$^{-/-}$ *Ku70*$^{-/-}$ mice, and apoptosis levels were similar to those observed in *Ku70*$^{-/-}$ cells (Fig. 5B,C), but lower than those observed in *Snm1B/Apollo*$^{-/-}$ cells (Fig. 2B). These findings indicate that the abrogation of NHEJ rescues the defects in *Snm1B/Apollo*$^{-/-}$ mice consistent with the reduced telomeric end-joining observed in *Snm1B/Apollo*$^{-/-}$ *Ku70*$^{-/-}$ MEFs as we have reported elsewhere (Lam *et al.*, 2010). In all notable respects, except the one discussed below, the *Ku70*$^{-/-}$ mice and the *Snm1B/Apollo*$^{-/-}$ *Ku70*$^{-/-}$ mice were

phenotypically indistinct, and somewhat surprisingly, there were no differences in cancer incidence, which was not elevated in either strain. One minor difference that we noted between the *Snm1B/Apollo*$^{-/-}$ *Ku70*$^{-/-}$ and the *Ku70*$^{-/-}$ mice was that the former exhibited black paws and tails (Fig. 5A). Interestingly, such a phenotype has been reported in mice with mutations in ribosomal proteins leading to the stabilization of p53 and consequent upregulation of Kit ligand expression and epidermal melanocytosis (McGowan *et al.*, 2008). In addition, several mouse models with telomere dysfunction have also been reported to exhibit hyperpigmentation (Munoz *et al.*, 2005; Martinez *et al.*, 2009). Thus, it is likely that the absence of *SNM1B/Apollo* leads to damaged telomeres and the subsequent stabilization of p53.

Discussion

In this report, we have described the physiological consequences of a disruption of *SNM1B/Apollo* in a mouse model. *Snm1B/Apollo* null embryos died immediately after birth as a result of multi-organ developmental failure leading to an inability to survive outside the womb. Cellular studies on MEFs in culture and examination of tissues showed that *Snm1B/Apollo*$^{-/-}$ cells had reduced proliferation capacity and increased apoptosis compared to wild-type or heterozygous littermates. These defects are the likely causes of the observed multi-organ developmental failure. We also showed that absence of SNM1B/Apollo led to an elevated level of chromosome end-to-end fusions, thus confirming the role for SNM1B/Apollo in telomere protection. In a separate report (Lam *et al.*, 2010), we have characterized in detail the molecular mechanism responsible for the increased chromosomal fusions. SNM1B/Apollo possesses a 5′–3′ exonuclease activity, and we showed that this activity is required to generate 3′ single-stranded overhangs at telomeres formed by leading-strand replicative synthesis. Generation of 3′ single-stranded overhangs is required for the formation of protective structures (t-loops) at the telomere, which prevent the activation of the DDR and the resulting chromosomal end-to-end fusion (Longhese, 2008). Thus, we propose that the disruption of *SNM1B/Apollo* leads to elevated chromosomal fusions and the accompanying genomic instability, which in turn causes cellular proliferation defects and developmental organ failure. In support of this model, we showed that a cross with *Ku70* null mice resulted in the rescue of the perinatal lethality because of the genomic disruption of *SNM1B/Apollo*. Ku70 is a core component of the NHEJ pathway, and abrogation of this DSB repair pathway in *Snm1B/Apollo*$^{-/-}$ *Ku70*$^{-/-}$ cells led to greatly reduced chromosomal end-to-end fusions compared to *Snm1B/Apollo*$^{-/-}$ cells (Lam *et al.*, 2010). Thus, in the absence of NHEJ, the deprotection of telomeres caused by the absence of *SNM1B/Apollo* does not result in increased genomic instability and the resulting organ failure. It is interesting to note that the developmental deficiencies of *Snm1B/Apollo* null mice do not appear as severe at early stages because the embryos at E11.5 show only moderate growth reduction (Fig. 1A). This result may be explained by reported findings indicating that homologous recombination as opposed to NHEJ is the primary pathway of DSB repair during the early stages of mouse development (Orii *et al.*, 2006).

Also of interest was our finding that a knockout of *p53* was unable to rescue the perinatal lethality found in *Snm1B/Apollo* null mice indicating that p53-dependent apoptosis was not responsible for the observed defects in cellular proliferation. This finding was surprising in light of a recent report in which a conditional knockout of the telomere-binding protein TRF1, which induced perinatal lethality, was rescued by p53 deficiency (Martinez *et al.*, 2009). The TRF1-deficient cells exhibited increased telomere damage similar to that observed in *Snm1B/Apollo*$^{-/-}$ cells. As the conditional TRF1 knockout was induced only in stratified epithelia, and did not affect other organ systems, it is possible that this particular cell type was subject to rescue by p53 deficiency, whereas the whole animal knockout of SNM1B/Apollo was not capable of rescue. A knockout of ATM also did not rescue *Snm1B/*

Apollo null mice indicating that the NHEJ pathway responsible for the chromosomal end-to-end joining was not dependent upon this kinase (Lam *et al.*, 2010). This finding is interesting in light of the fact that at least some forms of DSBs are dependent upon ATM for their repair (Adams *et al.*, 2010; Suzuki *et al.*, 2010).

Our studies on a knockout model of *SNM1B/Apollo* in the mouse have led to a further understanding of its role in telomere biology. Its 5′–3′ exonuclease activity is required to resect the newly synthesized leading strand at telomeres to form the t-loop protective structures (Lam *et al.*, 2010). In the absence of SNM1B/Apollo, genomic instability occurs causing multi-organ failure and perinatal lethality. While the null genotype results in lethality in mice, it is distinctly possible that somatic mutations of *SNM1B/Apollo* could lead to cancer or other diseases in humans. In fact, while this paper was in preparation, it was reported (Touzot *et al.*, 2010) that a splice variant of SNM1B/Apollo lacking the TRF2-binding domain was found in patients with Hoyeraal–Hreidarsson syndrome, a disease characterized by premature aging, bone marrow failure, and immunodeficiency. This splice variant led to telomere dysfunction and cellular senescence confirming the role of SNM1B/Apollo in telomere maintenance in humans.

Experimental procedures

Generation of mice

Generation of *Snm1B/Apollo* knockout mice by disruption of exon 4 was described elsewhere (Lam *et al.*, 2010). To generate double mutants of *Snm1B/Apollo* and Trp53 or Ku70, Snm1B/Apollo$^{-/+}$ mice were crossed with Trp53$^{-/-}$ (129/C57BL; kindly provided by Guillermina Lozano), *or Ku70*$^{-/-}$ *mice*, which were then bred to generate all cohort mice. Genotyping for *Trp53* and *Ku70* was performed by PCR as described previously (Jacks *et al.*, 1994; Li *et al.*, 2007).

Mouse handling

All mice were maintained according to NIH guidelines and an approved Animal Care and Use Committee protocol. Mice used in this study were housed in conventional specific pathogen-free facility and were regularly monitored.

Embryo collection, histology, and morphometric analysis

Embryos at stage E13.5 were used to generate MEFs. For morphometric analysis, different stages of embryos were collected and fixed, and embedded according to a standard protocol. Sagittal step sections were performed every 100 μm, and 5-μm sections were stained with hematoxylin and eosin (H&E). Tissues were analyzed by light microscopy.

Proliferation assay

To monitor proliferation, MEF cells were maintained on a defined 3-day passage schedule by plating 3×10^5 cells (3T3 protocol) in 60-mm dishes as described previously (Todaro & Green, 1963). The cells were counted at each passage, and the total number was calculated prior to replating. Growth rates at passage 2 were determined by plating replicate cultures of 2.5×10^4 cells in 35-mm dishes. Triplicate cultures were harvested every day thereafter, and cells were counted. To measure the fraction of cells in S phase, cells, at passage 3, were briefly exposed to 5-bromo-2′-deoxyuridine (BrdU); subsequently, cells were stained with *In Situ* Cell Proliferation kit, FLUOS (Roche, Indianapolis, IN, USA). To label replicated DNA in embryos, mothers carrying 14-day-old embryos were injected with BrdU (Zymed, San Francisco, CA, USA). Two hours later, the animals were sacrificed and the embryos were collected. Embryos were then processed for paraffin embedding, and sections were immunostained with anti-BrdU antibody.

Chromosome analysis: cytological preparation and fluorescence *in situ* hybridization (FISH)

Chromosome analyses were performed as described previously (Multani *et al.*, 2000). At least 35 metaphases were analyzed from each sample for chromosome aberrations. For FISH analysis, cytological preparation of both wild-type and *Snm1/Apollo* homozygous MEF cells were hybridized with a human telomeric DNA probe.

Supplementary Material

Refer to Web version on PubMed Central for supplementary material.

Acknowledgments

We thank Asha Multani for carrying out the chromosome analyses. RJL acknowledges support by NCI grants (CA052461 and CA097175). SC acknowledges generous financial support from the NIA (RO1 AG028888), the NCI (RO1 CA129037), the Welch Foundation, the Susan G Koman Race for the Cure Foundation, the Abraham and Phyllis Katz Foundation, and the Michael Kadoorie Cancer Genetics Research Program.

References

Adams BR, Golding SE, Rao RR, Valerie K. Dynamic dependence on ATR and ATM for double-strand break repair in human embryonic stem cells and neural descendants. PLoS ONE. 2010; 5:e10001. [PubMed: 20368801]

Ahkter S, Richie CT, Zhang N, Behringer RR, Zhu C, Legerski RJ. Snm1-deficient mice exhibit accelerated tumorigenesis and susceptibility to infection. Mol. Cell. Biol. 2005; 25:10071–10078. [PubMed: 16260620]

Akhter S, Legerski RJ. SNM1A acts downstream of ATM to promote the G1 cell cycle checkpoint. Biochem. Biophys. Res. Commun. 2008; 377:236–241. [PubMed: 18848520]

Akhter S, Richie CT, Deng JM, Brey E, Zhang X, Patrick C Jr, Behringer RR, Legerski RJ. Deficiency in SNM1 abolishes an early mitotic checkpoint induced by spindle stress. Mol. Cell. Biol. 2004; 24:10448–10455. [PubMed: 15542852]

Bae JB, Mukhopadhyay SS, Liu L, Zhang N, Tan J, Akhter S, Liu X, Shen X, Li L, Legerski RJ. Snm1B/Apollo mediates replication fork collapse and S Phase checkpoint activation in response to DNA interstrand cross-links. Oncogene. 2008; 27:5045–5056. [PubMed: 18469862]

Barber LJ, Ward TA, Hartley JA, McHugh PJ. DNA interstrand cross-link repair in the Saccharomyces cerevisiae cell cycle: overlapping roles for PSO2 (SNM1) with MutS factors and EXO1 during S phase. Mol. Cell. Biol. 2005; 25:2297–2309. [PubMed: 15743825]

Beucher A, Birraux J, Tchouandong L, Barton O, Shibata A, Conrad S, Goodarzi AA, Krempler A, Jeggo PA, Lobrich M. ATM and Artemis promote homologous recombination of radiation-induced DNA double-strand breaks in G2. EMBO J. 2009; 28:3413–3427. [PubMed: 19779458]

Callebaut I, Moshous D, Mornon JP, de Villartay JP. Metallo-beta-lactamase fold within nucleic acids processing enzymes: the beta-CASP family. Nucleic Acids Res. 2002; 30:3592–3601. [PubMed: 12177301]

Cattell E, Sengerova B, McHugh PJ. The SNM1/Pso2 family of ICL repair nucleases: from yeast to man. Environ. Mol. Mutagen. 2010; 51:491–668. [PubMed: 20577999]

Chen Y, Yang Y, van Overbeek M, Donigian JR, Baciu P, de Lange T, Lei M. A shared docking motif in TRF1 and TRF2 used for differential recruitment of telomeric proteins. Science. 2008; 319:1092–1096. [PubMed: 18202258]

Demuth I, Digweed M, Concannon P. Human SNM1B is required for normal cellular response to both DNA interstrand crosslink-inducing agents and ionizing radiation. Oncogene. 2004; 23:8611–8618. [PubMed: 15467758]

Demuth I, Bradshaw PS, Lindner A, Anders M, Heinrich S, Kallenbach J, Schmelz K, Digweed M, Meyn MS, Concannon P. Endogenous hSNM1B/Apollo interacts with TRF2 and stimulates ATM in response to ionizing radiation. DNA Repair (Amst). 2008; 7:1192–1201. [PubMed: 18468965]

Denchi EL, de Lange T. Protection of telomeres through independent control of ATM and ATR by TRF2 and POT1. Nature. 2007; 448:1068–1071. [PubMed: 17687332]

Dronkert ML, de Wit J, Boeve M, Vasconcelos ML, van Steeg H, Tan TL, Hoeijmakers JH, Kanaar R. Disruption of mouse SNM1 causes increased sensitivity to the DNA interstrand cross-linking agent mitomycin C. Mol. Cell. Biol. 2000; 20:4553–4561. [PubMed: 10848582]

Freibaum BD, Counter CM. hSnm1B is a novel telomere-associated protein. J. Biol. Chem. 2006; 281:15033–15036. [PubMed: 16606622]

Gao Y, Ferguson DO, Xie W, Manis JP, Sekiguchi J, Frank KM, Chaudhuri J, Horner J, DePinho RA, Alt FW. Interplay of p53 and DNA-repair protein XRCC4 in tumorigenesis, genomic stability and development. Nature. 2000; 404:897–900. [PubMed: 10786799]

Geng L, Zhang X, Zheng S, Legerski RJ. Artemis links ATM to G2/M checkpoint recovery via regulation of Cdk1-cyclin B. Mol. Cell. Biol. 2007; 27:2625–2635. [PubMed: 17242184]

Guo X, Deng Y, Lin Y, Cosme-Blanco W, Chan S, He H, Yuan G, Brown EJ, Chang S. Dysfunctional telomeres activate an ATM-ATR-dependent DNA damage response to suppress tumorigenesis. EMBO J. 2007; 26:4709–4719. [PubMed: 17948054]

Hazrati A, Ramis-Castelltort M, Sarkar S, Barber LJ, Schofield CJ, Hartley JA, McHugh PJ. Human SNM1A suppresses the DNA repair defects of yeast pso2 mutants. DNA Repair (Amst). 2008; 7:230–238. [PubMed: 18006388]

Hejna J, Philip S, Ott J, Faulkner C, Moses R. The hSNM1 protein is a DNA 5′-exonuclease. Nucleic Acids Res. 2007; 35:6115–6123. [PubMed: 17804464]

Henriques JA, Moustacchi E. Isolation and characterization of pso mutants sensitive to photo-addition of psoralen derivatives in Saccharomyces cerevisiae. Genetics. 1980; 95:273–288. [PubMed: 7009316]

Jacks T, Remington L, Williams BO, Schmitt EM, Halachmi S, Bronson RT, Weinberg RA. Tumor spectrum analysis in p53-mutant mice. Curr. Biol. 1994; 4:1–7. [PubMed: 7922305]

Lam YC, Akhter S, Gu P, Ye J, Poulet A, Giraud-Panis MJ, Bailey SM, Gilson E, Legerski RJ, Chang S. SNMIB/Apollo protects leading-strand telomeres against NHEJ-mediated repair. EMBO J. 2010; 29:2230–2241. [PubMed: 20551906]

de Lange T. Shelterin: the protein complex that shapes and safeguards human telomeres. Genes Dev. 2005; 19:2100–2110. [PubMed: 16166375]

Lenain C, Bauwens S, Amiard S, Brunori M, Giraud-Panis MJ, Gilson E. The Apollo 5′ exonuclease functions together with TRF2 to protect telomeres from DNA repair. Curr. Biol. 2006; 16:1303–1310. [PubMed: 16730175]

Li X, Moses RE. The beta-lactamase motif in Snm1 is required for repair of DNA double-strand breaks caused by interstrand crosslinks in S. cerevisiae. DNA Repair (Amst). 2003; 2:121–129. [PubMed: 12509272]

Li X, Hejna J, Moses RE. The yeast Snm1 protein is a DNA 5′-exonuclease. DNA Repair (Amst). 2005; 4:163–170. [PubMed: 15590324]

Li H, Vogel H, Holcomb VB, Gu Y, Hasty P. Deletion of Ku70, Ku80, or both causes early aging without substantially increased cancer. Mol. Cell. Biol. 2007; 27:8205–8214. [PubMed: 17875923]

Liu L, Akhter S, Bae JB, Mukhopadhyay SS, Richie CT, Liu X, Legerski R. SNM1B/Apollo interacts with astrin and is required for the prophase cell cycle checkpoint. Cell Cycle. 2009; 8:628–638. [PubMed: 19197158]

Longhese MP. DNA damage response at functional and dysfunctional telomeres. Genes Dev. 2008; 22:125–140. [PubMed: 18198332]

Ma Y, Pannicke U, Schwarz K, Lieber MR. Hairpin opening and overhang processing by an Artemis/DNA-dependent protein kinase complex in nonhomologous end joining and V(D)J recombination. Cell. 2002; 108:781–794. [PubMed: 11955432]

Magana-Schwencke N, Henriques JA, Chanet R, Moustacchi E. The fate of 8-methoxypsoralen photoinduced crosslinks in nuclear and mitochondrial yeast DNA: comparison of wild-type and repair-deficient strains. Proc. Natl Acad. Sci. USA. 1982; 79:1722–1726. [PubMed: 6281782]

Martinez P, Thanasoula M, Munoz P, Liao C, Tejera A, McNees C, Flores JM, Fernandez-Capetillo O, Tarsounas M, Blasco MA. Increased telomere fragility and fusions resulting from TRF1 deficiency

lead to degenerative pathologies and increased cancer in mice. Genes Dev. 2009; 23:2060–2075. [PubMed: 19679647]

McGowan KA, Li JZ, Park CY, Beaudry V, Tabor HK, Sabnis AJ, Zhang W, Fuchs H, de Angelis MH, Myers RM, Attardi LD, Barsh GS. Ribosomal mutations cause p53-mediated dark skin and pleiotropic effects. Nat. Genet. 2008; 40:963–970. [PubMed: 18641651]

Moshous D, Callebaut I, de Chasseval R, Corneo B, Cavazzana-Calvo M, Le Deist F, Tezcan I, Sanal O, Bertrand Y, Philippe N, Fischer A, de Villartay JP. Artemis, a novel DNA double-strand break repair/V(D)J recombination protein, is mutated in human severe combined immune deficiency. Cell. 2001; 105:177–186. [PubMed: 11336668]

Multani AS, Ozen M, Narayan S, Kumar V, Chandra J, McConkey DJ, Newman RA, Pathak S. Caspase-dependent apoptosis induced by telomere cleavage and TRF2 loss. Neoplasia. 2000; 2:339–345. [PubMed: 11005568]

Munoz P, Blanco R, Flores JM, Blasco MA. XPF nuclease-dependent telomere loss and increased DNA damage in mice overexpressing TRF2 result in premature aging and cancer. Nat. Genet. 2005; 37:1063–1071. [PubMed: 16142233]

Orii KE, Lee Y, Kondo N, McKinnon PJ. Selective utilization of nonhomologous end-joining and homologous recombination DNA repair pathways during nervous system development. Proc. Natl Acad. Sci. USA. 2006; 103:10017–10022. [PubMed: 16777961]

van Overbeek M, de Lange T. Apollo, an Artemis-related nuclease, interacts with TRF2 and protects human telomeres in S phase. Curr. Biol. 2006; 16:1295–1302. [PubMed: 16730176]

Pannicke U, Ma Y, Hopfner KP, Niewolik D, Lieber MR, Schwarz K. Functional and biochemical dissection of the structure-specific nuclease ARTEMIS. EMBO J. 2004; 23:1987–1997. [PubMed: 15071507]

Povirk LF, Zhou T, Zhou R, Cowan MJ, Yannone SM. Processing of 3′-phosphoglycolate-terminated DNA double strand breaks by Artemis nuclease. J. Biol. Chem. 2007; 282:3547–3558. [PubMed: 17121861]

Riballo E, Kuhne M, Rief N, Doherty A, Smith GC, Recio MJ, Reis C, Dahm K, Fricke A, Krempler A, Parker AR, Jackson SP, Gennery A, Jeggo PA, Lobrich M. A pathway of double-strand break rejoining dependent upon ATM, Artemis, and proteins locating to gamma-H2AX foci. Mol. Cell. 2004; 16:715–724. [PubMed: 15574327]

Ruhland A, Kircher M, Wilborn F, Brendel M. A yeast mutant specifically sensitive to bifunctional alkylation. Mutat. Res. 1981; 91:457–462. [PubMed: 7027037]

Scholzen T, Gerdes J. The Ki-67 protein: from the known and the unknown. J. Cell. Physiol. 2000; 182:311–322. [PubMed: 10653597]

Suzuki K, Takahashi M, Oka Y, Yamauchi M, Suzuki M, Yamashita S. Requirement of ATM-dependent pathway for the repair of a subset of DNA double strand breaks created by restriction endonucleases. Genome Integr. 2010; 1:4. [PubMed: 20678255]

Todaro GJ, Green H. Quantitative studies of the growth of mouse embryo cells in culture and their development into established lines. J. Cell Biol. 1963; 17:299–313. [PubMed: 13985244]

Touzot F, Callebaut I, Soulier J, Gaillard L, Azerrad C, Durandy A, Fischer A, de Villartay JP, Revy P. Function of Apollo (SNM1B) at telomere highlighted by a splice variant identified in a patient with Hoyeraal-Hreidarsson syndrome. Proc. Natl Acad. Sci. USA. 2010; 107:10097–10102. [PubMed: 20479256]

Weterings E, Verkaik NS, Keijzers G, Florea BI, Wang SY, Ortega LG, Uematsu N, Chen DJ, van Gent DC. The Ku80 carboxy terminus stimulates joining and artemis-mediated processing of DNA ends. Mol. Cell. Biol. 2009; 29:1134–1142. [PubMed: 19103741]

Wilborn F, Brendel M. Formation and stability of interstrand cross-links induced by cis- and trans-diamminedichloroplatinum (II) in the DNA of Saccharomyces cerevisiae strains differing in repair capacity. Curr. Genet. 1989; 16:331–338. [PubMed: 2692851]

Yan Y, Akhter S, Zhang X, Legerski R. The multifunctional SNM1 gene family: not just nucleases. Future Oncol. 2010; 6:1015–1029. [PubMed: 20528238]

Yannone SM, Khan IS, Zhou RZ, Zhou T, Valerie K, Povirk LF. Coordinate 5′ and 3′ endonucleolytic trimming of terminally blocked blunt DNA double-strand break ends by Artemis

nuclease and DNA-dependent protein kinase. Nucleic Acids Res. 2008; 36:3354–3365. [PubMed: 18440975]

Zhang X, Succi J, Feng Z, Prithivirajsingh S, Story MD, Legerski RJ. Artemis is a phosphorylation target of ATM and ATR and is involved in the G2/M DNA damage checkpoint response. Mol. Cell. Biol. 2004; 24:9207–9220. [PubMed: 15456891]

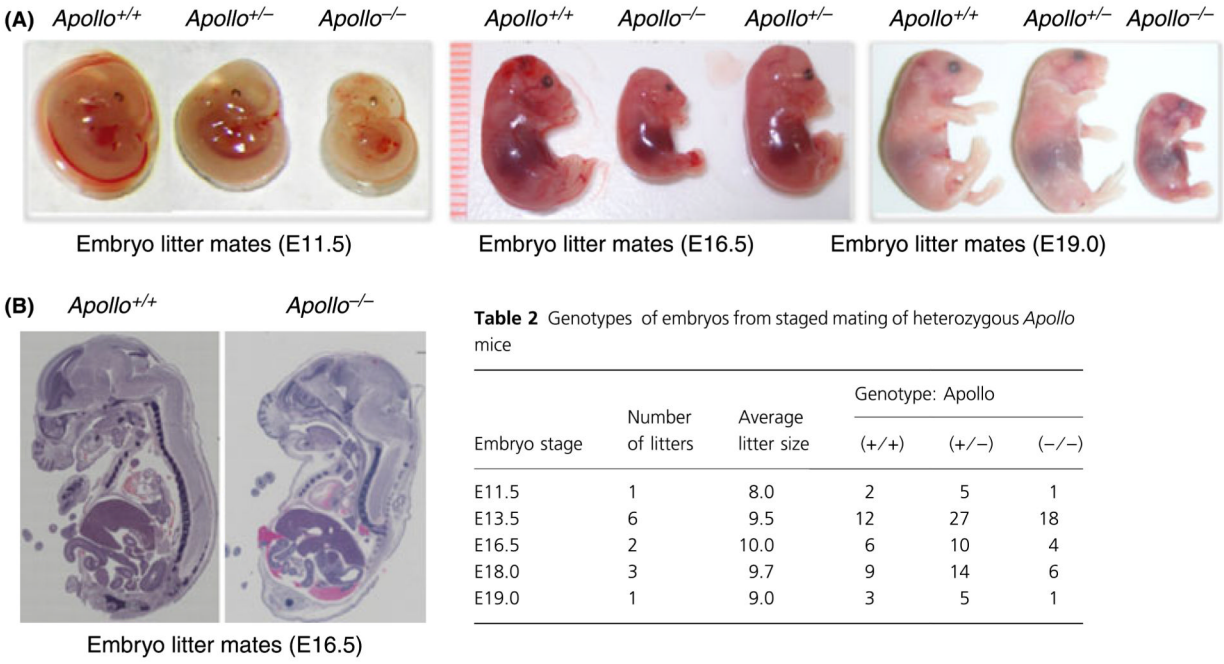

Table 2 Genotypes of embryos from staged mating of heterozygous *Apollo* mice

Embryo stage	Number of litters	Average litter size	Genotype: Apollo (+/+)	(+/–)	(–/–)
E11.5	1	8.0	2	5	1
E13.5	6	9.5	12	27	18
E16.5	2	10.0	6	10	4
E18.0	3	9.7	9	14	6
E19.0	1	9.0	3	5	1

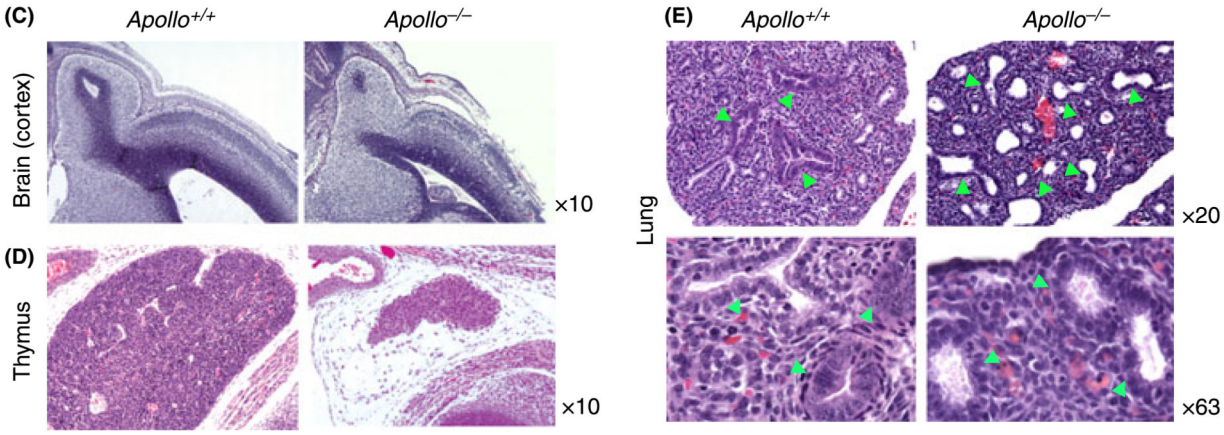

Fig. 1.

Knockout of *Snm1B/Apollo* causes developmental abnormalities. (A) Gross morphology of E11.5, E16.5, and E19 embryo littermates. (B) H&E-stained histological sections of E16.5 *Snm1B/Apollo* embryos (wild-type and homozygous). (C–E) H&E-stained histological sections of brain, lung, and thymus from E16.5 wild-type and homozygous *Snm1B/Apollo* embryos.

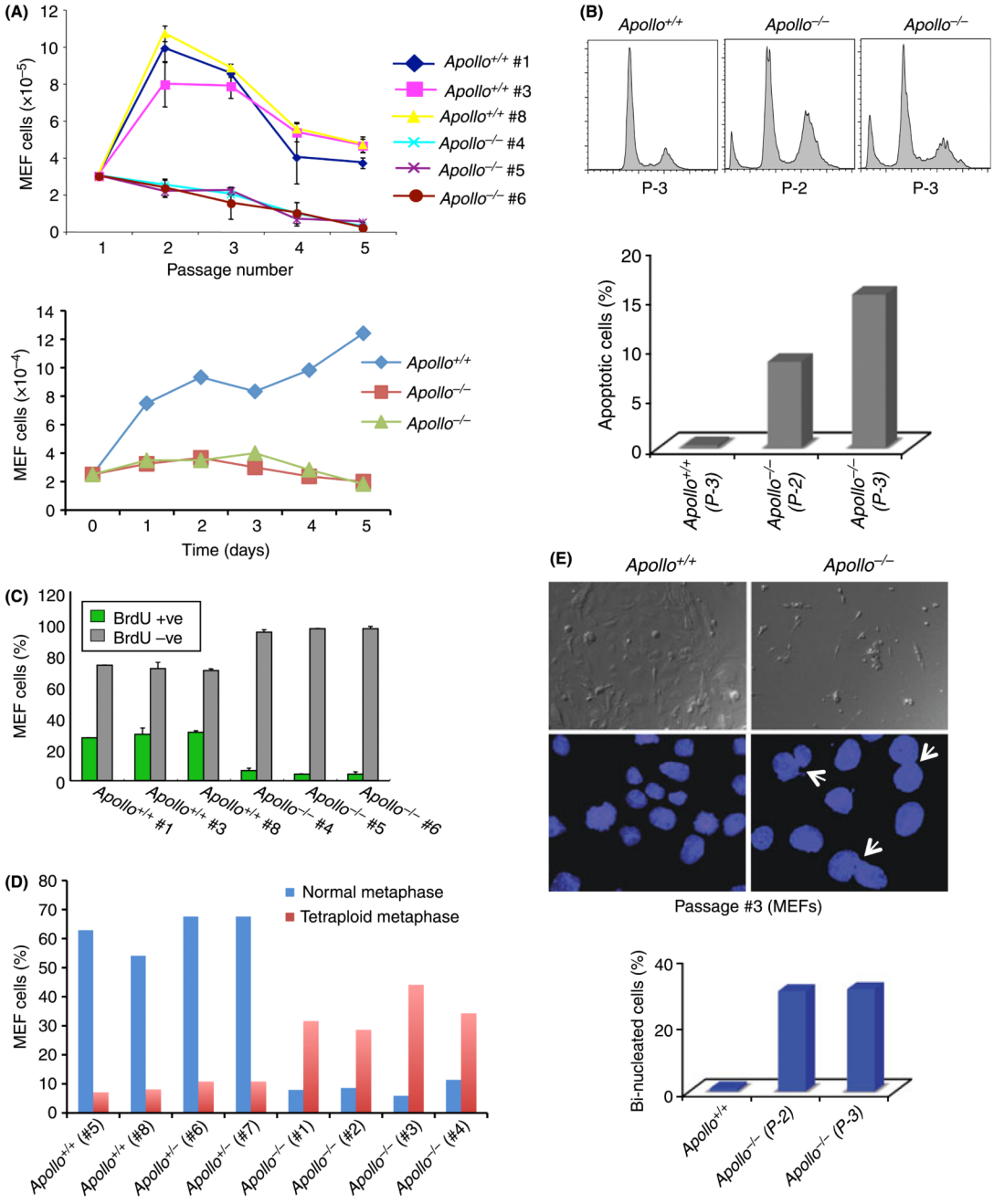

Fig. 2.

Knockout of *Snm1B/Apollo* causes proliferation defects in mouse embryonic fibroblasts (MEFs). (A) Cellular growth was followed by the 3T3 protocol (upper panel), and proliferation rates were determined for passage 2 *Snm1B/Apollo* MEFs (lower panel). MEFs by embryo number and genotypes are as indicated in the graphs. (B) *Snm1B/Apollo*$^{-/-}$ MEFs exhibit increased apoptosis as indicated by FACS analysis showing an elevated subG1 population. (C) The S-phase population is reduced in *Snm1B/Apollo*$^{-/-}$ MEFs as indicated by BrdU incorporation in passage 3 cells. (D) Quantitation of abnormal metaphases in passage 3 *Snm1B/Apollo*$^{-/-}$ MEFs. (E) Quantitation of binucleated cells by DAPI staining in passage 3 *Snm1B/Apollo*$^{-/-}$ MEFs.

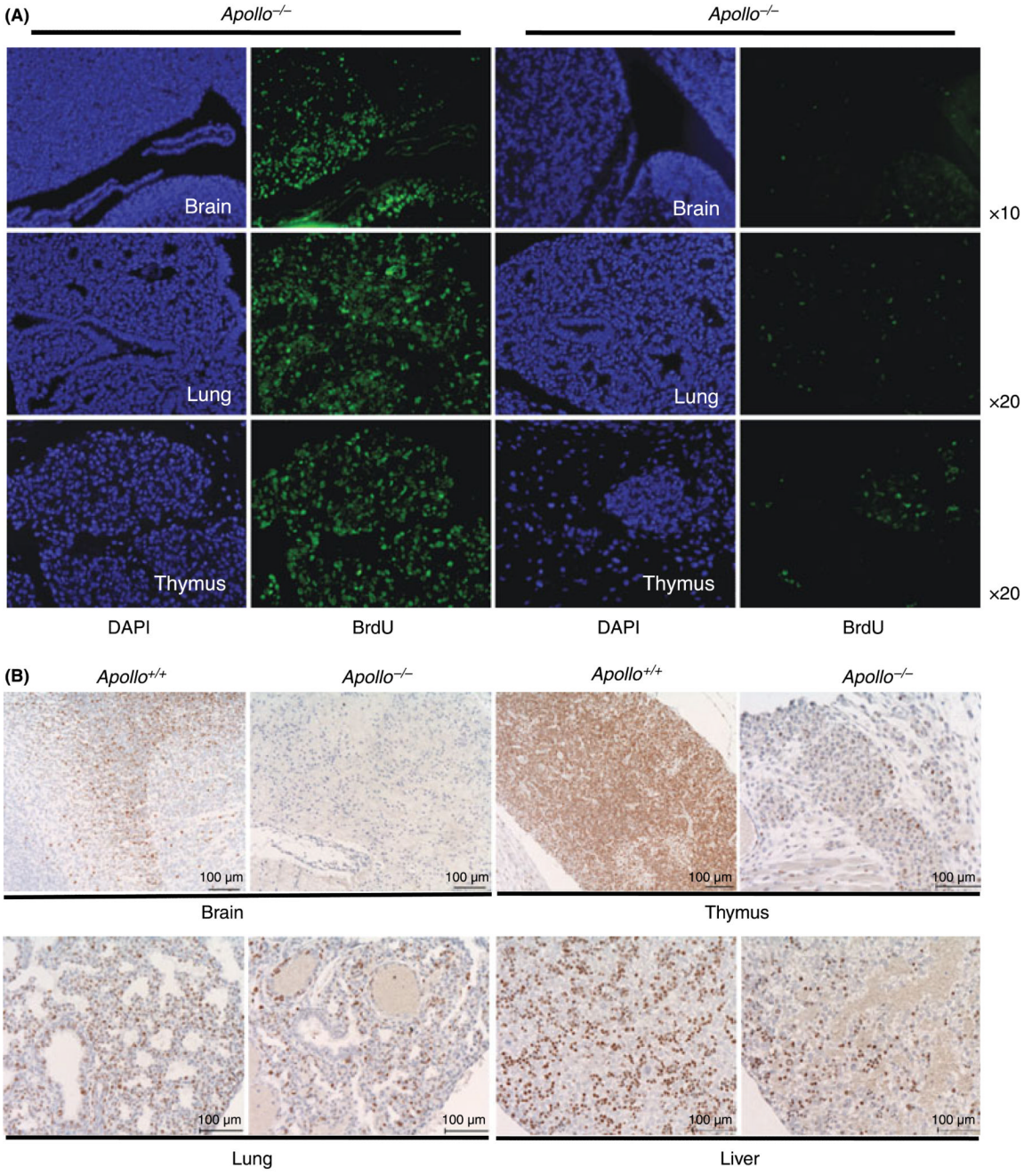

Fig. 3.

Cell proliferation of *Snm1B/Apollo* embryos was examined in different organs. (A) Cell proliferation measured by immunostaining for BrdU in the indicated organs (E14). (B) Immunostaining for the proliferation marker Ki-67 in the indicated organs (E16.5).

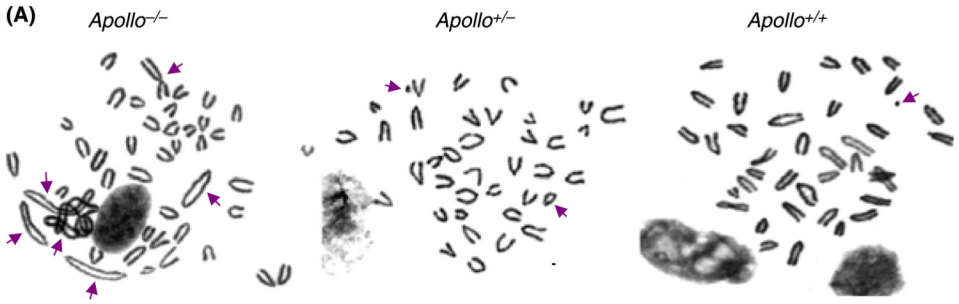

(B)

MEFs	% Aberrant metaphase	% Cells with breaks	% Cells with fusions
Apollo$^{+/+}$ (#5)	28.6	11.4	8.6
Apollo$^{+/+}$ (#8)	32.4	18.9	16.2
Apollo$^{+/-}$ (#6)	21.6	13.5	5.4
Apollo$^{+/-}$ (#7)	18.9	8.1	8.1
Apollo$^{-/-}$ (#1)	89.5	36.8	68.4
Apollo$^{-/-}$ (#2)	91.4	31.4	88.6
Apollo$^{-/-}$ (#3)	91.2	29.4	88.2
Apollo$^{-/-}$ (#4)	85.7	14.3	77.1

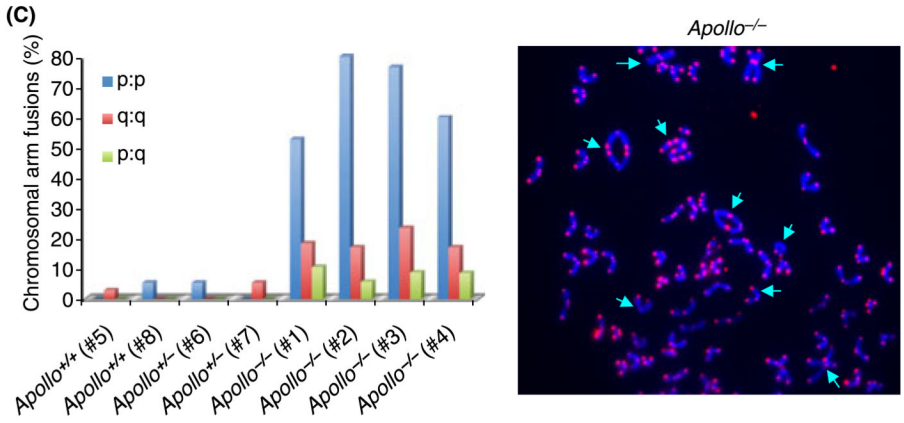

Fig. 4.

Knockout of *Snm1B/Apollo* increases chromosomal instability in mouse embryonic fibroblasts (MEFs). (A) Metaphase chromosomes are shown from primary MEF cultures (passage 2). Arrows indicate fused chromosomes. (B) Quantitation of aberrant metaphases shown in (A). (C) *Snm1B/Apollo*$^{-/-}$ mutant MEFs exhibit elevated levels of telomeric fusions as shown by a FISH assay. Arrows indicate fused chromosomes (right panel). The graph shows a summary of the frequency of chromosomal aberrations in early-passage MEFs. Short and long chromosomal arms are indicated by p and q, respectively.

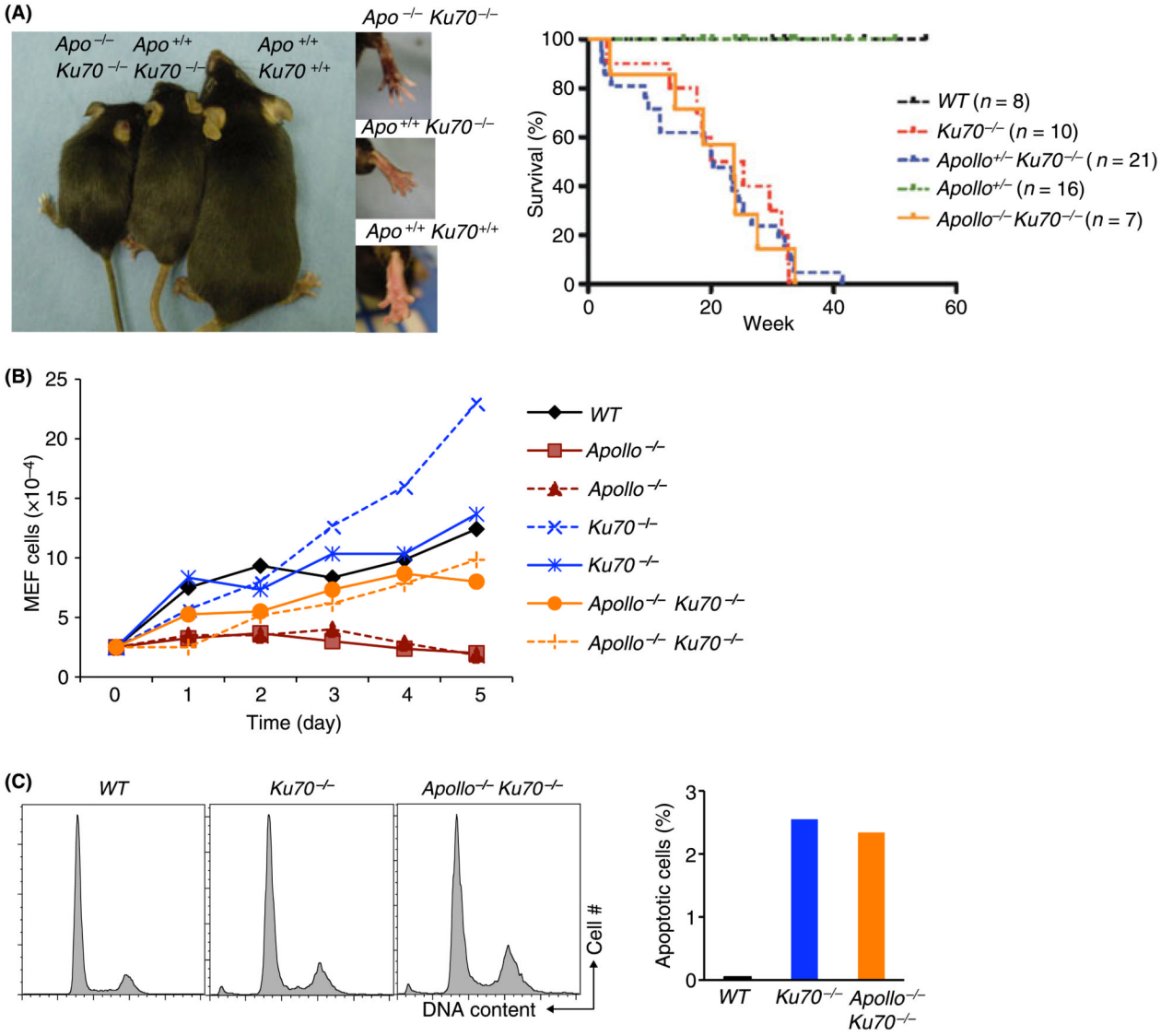

Fig. 5.

Knockout of Ku70 rescues the *Snm1B/Apollo*$^{-/-}$ phenotype. (A) *Snm1B/Apollo*$^{-/-}$ *Ku70*$^{-/-}$ mice are viable and approximately the size of *Ku70*$^{-/-}$ mice (left panel). The survival of *Snm1B/Apollo*$^{-/-}$ *Ku70*$^{-/-}$ mice is comparable to *Ku70*$^{-/-}$ mice as shown by Kaplan–Meier analysis (right panel). (B) Growth of *Snm1B/Apollo*$^{-/-}$ *Ku70*$^{-/-}$ primary mouse embryonic fibroblasts (MEFs) is similar to *Ku70*$^{-/-}$ primary MEFs as indicated in a proliferation assay. (C) Cell cycle analysis by FACS indicates that the level of apoptosis as shown by the sub-G1 population is similar between *Snm1B/Apollo*$^{-/-}$ *Ku70*$^{-/-}$ MEFs and *Ku70*$^{-/-}$ MEFs.

Table 1

Genotypes of live progeny from intercrosses of heterozygous *SnmlB/Apollo* mice

Source*	Number of litters	Average litter size	Genotype: *Apollo*		
			(+/+)	(+/−)	(−/−)
F2	15	6.7	40	60	0
D6	21	7.6	62	97	0

*F2 and D6 represent two independent ES clones.

Table 2

Genotypes of embryos from staged mating of heterozygous *SnmlB/Apollo* mice

Embryo stage	Number of litters	Average litter size	Genotype: *Apollo*		
			(+/+)	(+/−)	(−/−)
E11.5	1	8.0	2	5	1
E13.5	6	9.5	12	27	18
E16.5	2	10.0	6	10	4
E18.0	3	9.7	9	14	6
E19.0	1	9.0	3	5	1

Aging Cell. Author manuscript; available in PMC 2013 July 23.